Vol 18 No 11, November 2009
1674-1056/2009/18(11)/4870-05

Chinese Physics B

© 2009 Chin. Phys. Soc.
and IOP Publishing Ltd

Analysis of waveguide structure for surface plasmon polariton interference*

Wang Jing-Quan(王景全)[a], Liang Hui-Min(梁慧敏)[b], Fang Liang(方 亮)[c], Li Min(李 敏)[a], Niu Xiao-Yun(牛晓云)[a], and Du Jing-Lei(杜惊雷)[a]†

[a] *Physics Department, Sichuan University, Chengdu* 610064, *China*

[b] *College of Science, Hebei University of Engineering, Hebei* 056038, *China*

[c] *Institute of Optics and Electronics, Chinese Academy of Sciences, Chengdu* 610209, *China*

(Received 10 January 2009; revised manuscript received 17 March 2009)

This paper describes a multi-reflected mode based on a narrow waveguide to enlarge the interferential area of surface plasmon polaritons (SPPs). A reasonable thickness of metal film is coated under the waveguide, the incident angle and the waveguide thickness are optimized in order to effectively increase interferential area. This is a key point for research into the Goos–Hänchen shift to optimize the waveguide thickness. Finally, the SPP interferential field is simulated with the finite-difference time-domain (FDTD) technique to prove the optimized results, and indicates that not only is the interferential area enlarged, but the high contrast is also maintained. Furthermore, the mode can fabricate some specific interferential patterns by adding some modulating techniques to the waveguide. So the mode has potential application in the fabrication of sub-wavelength patterns.

Keywords: surface plasmon polaritons (SPPs), sub-wavelength interferential lithography, waveguide, Goos–Hänchen shift

PACC: 4200, 7320J

1. Introduction

The interferential technique based on surface plasmon polaritons (SPPs) has been a hotspot in high-resolution lithography. Compared with extreme ultra-violet lithography[1] and the x-ray regime,[2,3] we find that SPP lithography has many advantages in fabrication, such as its simple scheme, high efficiency and low cost etc. At present, the surface plasmon (SP) resonant interference nanolithography technique[4] and SP interference nanolithography have been used to successfully fabricate a sub-100-nm interferential pattern.[5] However, both techniques are only suitable for small-area interference and need the fabrication of a mask grating with very fine periods. A simple but practical scheme based on the attenuated total reflection (ATR) coupling mode was designed to avoid fabricating the mask grating, and applied to large-area fabrication in our past work.[6,7] But the mode cannot excite large-area interference if the calibre of the incident beams is not large enough. Moreover, it is disadvantageous to form a special interferential pattern because it is difficult to modulate incident lights or interferential field.

In this paper, a multi-reflected mode is designed based on a narrow waveguide to compensate for the above-mentioned faults. Two incident light beams are reflected many times in the waveguide and form large-area SPPs interference. Furthermore, it is well-known that the waveguide takes on high flexibility, and some specific patterns can possibly be obtained by modulated techniques, such as waveguide variation or adding a mask on the waveguide surface. The optimization of the incident angle and the waveguide thickness is extremely important in order to gain a pattern of high quality in the mode because they determine the consistency of the phase and intensity at the interface between the waveguide and the metal film, and our work in this article focuses on a discussion of the two factors. At the end of this article, the SPP interferential field in the waveguide is simulated with the finite-difference time-domain (FDTD) technique, which indicates some perfect results.

*Project supported by the National Basic Research of China (Grant No 2006CD302902), the National Natural Science Foundation of China (Grant Nos 60676024 and 60878031) and the Specialized Research Fund of China for the Doctoral Program of Higher Education (Grant No 20060610006).

†Corresponding author. E-mail: dujl@scu.edu.cn

2. Analysis of the SPP interference based on ATR

In our past work, a scheme based on the ATR coupling mode was designed and analysed to get large-area interference,[6,7] and the mode is shown in Fig.1. The device comprises prism, metal film, photoresist and substrate. If the incident beams are TM waves, two SPP waves are excited under the metal film and form a sub-wavelength interferential pattern. Then, after the processes of exposure, development and fixation, the pattern can be transferred into the photoresist.

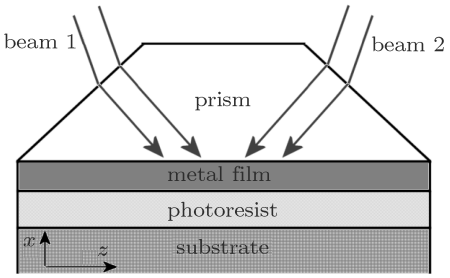


Fig.1. The ATR mode of the SPP interferential lithography.

The exposure is the result of a chemical reaction in the photoresist caused by the electric field E.[8,9] Therefore, it is necessary to analyse the electric field distribution in the lithography. In the lithography, the relation between electric field E and magnetic field H is expressed as

$$\begin{aligned} &E_y = H_x = H_z = 0, \\ &E^2 = E_x^2 + E_z^2 = \mu H_y^2/\varepsilon, \end{aligned} \tag{1}$$

where μ is the magnetic conductivity and ε is the dielectric coefficient. H_y is more convenient to use than E_x and E_z in the calculation and simulation because the electric field E includes two components E_x and E_z, and the magnetic field H only includes the component H_y.

The behaviours of the SPP interference are simulated with an FDTD technique. The parameters in the simulation are shown in Table 1. The SPP resonance is excited when the thickness of the silver film is 40 nm and the incident angle is 62°, as in the SPP interferential pattern shown in Fig.2. Figure 2(a) is the distribution of the interferential field. Figure 2(b) is the amplitude of H_y at the SPPs transmitting 5 nm vertically. It can be seen that the period of the interferential fringe is 128 nm, which shows that the critical dimension is 64 nm. Also, the pattern quality is very high in the middle of the figure.

Table 1. The parameters in the simulation.

parameters	values
incident wavelength/nm	441
refractive index of the prism	1.94325
refractive index of the photoresist	1.53
dielectric constant of silver	$-8.9170 + 0.2320$i

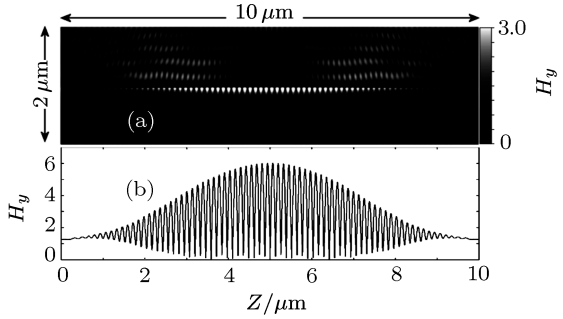


Fig.2. The SPP interferential patterns: (a) the interferential field; (b) the amplitude of H_y at the SPPs transmitting 5 nm vertically.

3. SPP interference modulation by a waveguide

The SPPs can be modulated flexibly by a waveguide to fabricate special patterns. In order to enlarge the SPP interferential area, a multi-reflected mode is designed based on a waveguide, as shown in Fig.3. The device comprises the rectangular waveguide, the metal film, the photoresist and the substrate, and the refractive indices are n_1, n_2, n_3 and n_4, respectively. The air refractive index is n_0. Two TM waves are irradiated from two sides of the waveguide and are reflected time after time. As a result, two large-area SPP fields are excited at the interface between the metal film and the photoresist. Thus the SPP interferential area is largely broadened. This is shown in our simulation.

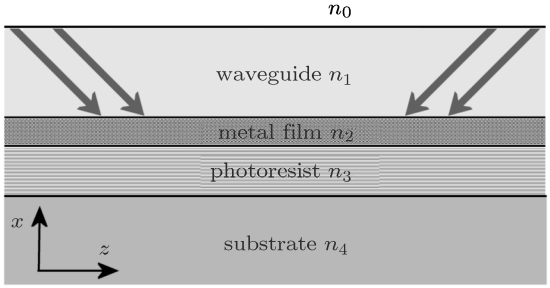


Fig.3. The waveguide mode of the SPP interference.

3.1. The optimization of the incident angle and the waveguide thickness

Although the waveguide mode can be applied to a large-area fabrication, many parameters must be optimized. The thickness of 40 nm silver film is an optimal parameter.[6,7] Besides, two parameters are important: one is the incident angl,; the other is the waveguide thickness. In the following the two parameters will be calculated and analysed in detail.

Firstly, it is well known that resonance of the SPPs is sensitive to the variation of the incident angle. The relation between the incident angle and the reflective index is simulated by the FDTD technique, shown in Fig.4. The parameters in the simulation are the same as the above-mentional ATR mode. The refractive index of the waveguide is equal to the prism, and the thickness of the silver film is 40 nm. The reflective index reaches a minimum value (approximately 19%) when the incident angle is 62° (the resonant angle), and it increases rapidly with the angle being shifted. If the incident angle is the resonant angle in the waveguide mode, the second reflection cannot excite the SPP waves whose intensity approximately equals the excitation of the first reflection, and thus large-area interference cannot be generated. Therefore, the resonant angle cannot be chosen as the incident angle in the waveguide mode. The energy of 75% is reflected after one reflection if the incident angle is 60°, and the light field is shown in Fig.5. The evanescent waves under the metal film are still enhanced to a certain extent. Estimated by the attenuation of the energy, the SPP waves can

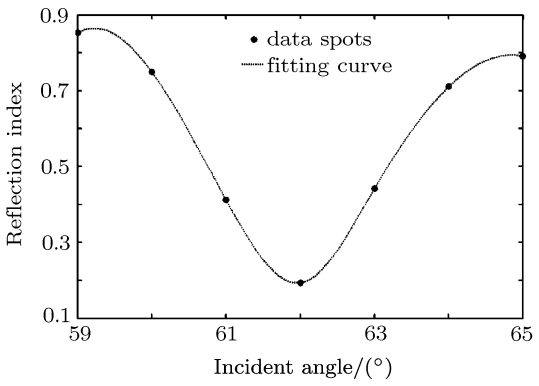


Fig.4. The relation between the reflective index and the incident angle.

be perfectly excited by three or four reflections at the interface between the waveguide and the metal film. The incident angle is temporarily selected in our design.

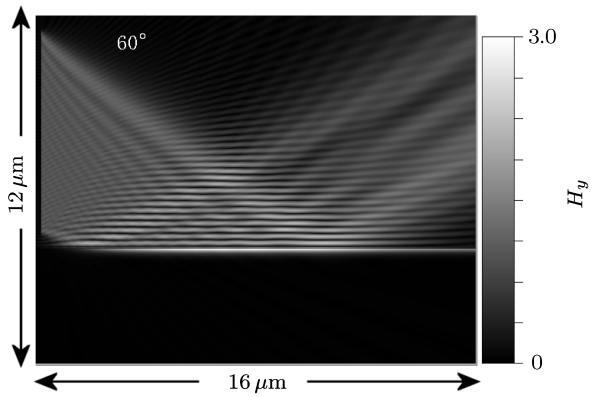


Fig.5. The light field distribution of the incident angle 60°.

Secondly, the waveguide thickness in the mode must be optimized because it influences the quality of the large-area interference. A random thickness probably causes an inconsistent intensity and phase at the interface between the waveguide and the metal film, which cannot make the interferential pattern even. Analysis and calculation of the Goos–Hänchen (GH) shift[10] is very important in the optimization as it determines the effective thickness of the waveguide.

At the interface between the waveguide and air (n_1/n_0), the GH shift is expressed as[11]

$$Z_1^{\mathrm{TM}} = \frac{n_0^2}{n_1^2 \sin^2\theta - n_0^2 \cos^2\theta} \cdot \frac{\tan\theta}{k_0\sqrt{n_1^2 \sin^2\theta - n_0^2}}, \quad (2)$$

where n_0 and n_1 are the refractive indices of the air and the waveguide, respectively. $k_0 = 2\pi/\lambda$, λ is the incident wavelength, θ is the incident angle.

The vertical shift is expressed as

$$X_1^{\mathrm{TM}} = Z_1^{\mathrm{TM}} \cos\theta. \quad (3)$$

At the surface between the waveguide and the metal film (n_1/n_2), the reflection coefficient is given as[12]

$$R = \frac{E_{\mathrm{r}}^{\mathrm{TM}}}{E_1^{\mathrm{TM}}} = \frac{r_{12}^{\mathrm{TM}} + r_{23}^{\mathrm{TM}} \exp(2\,\mathrm{i}\,k_{z2}d)}{1 + r_{12}^{\mathrm{TM}} r_{23}^{\mathrm{TM}} \exp(2\,\mathrm{i}\,k_{z2}d)} = |R| \exp(\mathrm{i}\,2\psi), \quad (4)$$

where

$$r_{lm}^{\mathrm{TM}} = \left(\frac{k_{zl}}{\varepsilon_l} - \frac{k_{zm}}{\varepsilon_m}\right) \Big/ \left(\frac{k_{zl}}{\varepsilon_l} + \frac{k_{zm}}{\varepsilon_m}\right), \quad (l = 1,\ 2,\ \ m = 2,\ 3), \quad (5)$$

k_{zl} and k_{zm} are the z direction components of the wave vectors, ε_l and ε_m are the dielectric coefficients of the different layers, 2ψ is the drift phase.

The GH shift at the interface is expressed as[11]

$$Z_2^{\mathrm{TM}} = \frac{1}{n_1 k_0 \cos\theta} \cdot \frac{\partial \psi}{\partial \theta}, \tag{6}$$

and the vertical shift is expressed as

$$X_2^{\mathrm{TM}} = Z_2^{\mathrm{TM}} \cos\theta. \tag{7}$$

Figure 6 illustrates the GH shifts at two interfaces shifting with the incident angle. The range of the incident angle is from 50° to 80° in the calculation, and other parameters are shown in Table 1. In addition, the thickness of the silver film is 40 nm. The figure shows that the shifts are positive at the interface of n_1/n_0 and negative at the interface of n_1/n_2, and two shifts are both small after one reflection.

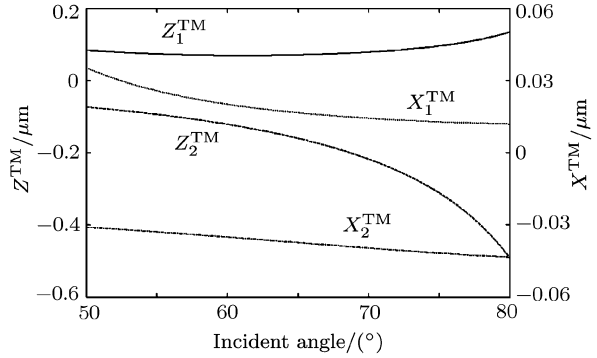


Fig.6. GH shifts shifting with the incident angle.

Supposing the waveguide thickness is d, we define the effective thickness D as

$$D = d + X_1^{\mathrm{TM}} + X_2^{\mathrm{TM}}. \tag{8}$$

After multi-reflections, if the consistent phase is generated at the interface between n_1/n_2, the following relation must be satisfied:

$$\frac{2D}{\cos\theta} = N\frac{\lambda}{n_1}, \quad (N = 1, 2, 3\ldots). \tag{9}$$

From Eqs.(8) and (9), we can deduce the waveguide thickness d as

$$d = N\frac{\lambda\cos\theta}{2n_1} - (X_1^{\mathrm{TM}} + X_2^{\mathrm{TM}}), \ (N = 1, 2, 3\ldots). \tag{10}$$

If the diffraction is not taken into account in the mode, then a waveguide with a thickness d calculated in Eq.(10) can generate a consistent phase at the interface between n_1/n_2. When the incident angle is 60°, the relation between d and N is shown in Fig.7.

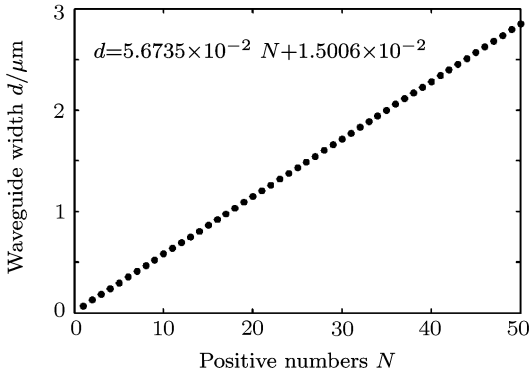


Fig.7. The relation between d and N at the incident angle 60°.

3.2. Simulation and analysis of SPP interference

The interferential field in the waveguide mode is simulated with the FDTD technique, and the result is shown in Fig.8. In the simulation, $N = 17$, that is $d = 0.98$ μm, the incident angle is 60°, the thickness of the silver film is 40 nm, and other parameters are shown in Table 1. Figure 8(a) is the amplitude distribution of the interferential field. Figure 8(b) is the amplitude of H_y at the SPPs transmitting 5 nm vertically. Compared with Fig.2, we find that the SPP interferential area is enlarged more than two times. The interferential period of the pattern is approximately 129 nm, that is, the critical dimension is 64.5 nm.

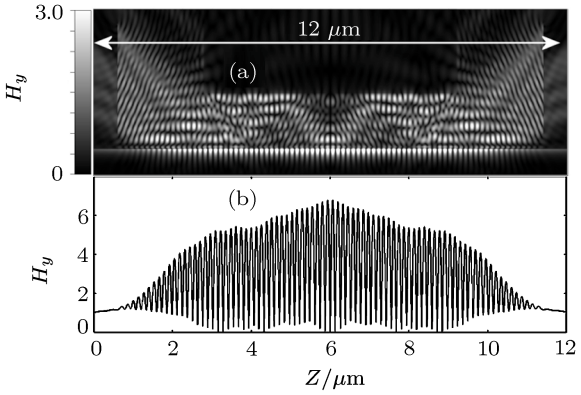


Fig.8. The SPP interferential simulation: (a) the interferential light field; (b) the amplitude of H_y distribution at the SPPs transmitting 5 nm vertically.

In order to exactly describe the pattern quality, the contrast is defined as

$$V = \frac{H_{y\max}^2 - H_{y\min}^2}{H_{y\max}^2 + H_{y\min}^2}, \tag{11}$$

where $H_{y\max}$ and $H_{y\min}$ are the maximum and the minimum of the amplitude in one period, respectively. The contrasts of 1 μm to 11 μm in Fig.8(b) are calculated, as shown in Fig.9. The contrasts are almost consistent from 2.5 μm to 9.5 μm, and more than 0.98.

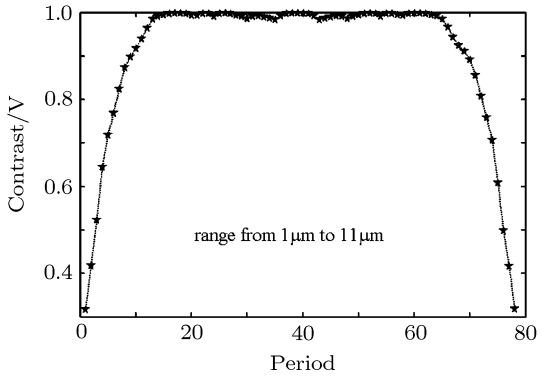


Fig.9. The contrast distribution at the SPPs transmitting 5 nm vertically.

4. Conclusion

A new scheme is designed for SPP interference based on a waveguide. The incident lights are reflected zigzag in the waveguide to enlarge SPP propagation length and form a large interference area. The incident angle and the waveguide thickness are analysed and optimized in detail because they influence the intensity and the phase distribution seriously at the interface between the waveguide and the metal film and the quality of the SPP interferential pattern. Finally, a large-area interferential pattern based on SPPs with high contrast is obtained by simulation of the FDTD technique. Of course, the reflected times in the waveguide are limited by some factors, such as energy attenuation and diffraction. In addition, the mode has another advantage that can design special sub-wavelength patterns by modulating techniques. So the mode has potential application in the fabrication of sub-wavelength patterns.

References

[1] Gwyn C W, Stulen R, Sweeney D and Attwood D 1998 *J. Vac. Sci. Technol.* B **16** 3142
[2] Silverman J P 1998 *J. Vac. Sci. Technol.* B **16** 3137
[3] Yi F T, Ye T C, Peng L Q, Chen D P, Zhang J F and Hand Y 2004 *Chin. Phys.* **13** 731
[4] Luo X G and Ishihara T 2004 *Appl. Phys. Lett.* **84** 4780
[5] Liu Z W, Wei Q H and Zhang X 2005 *Nano Lett.* **5** 957
[6] Guo X W, Du J L, Guo Y K and Yao J 2006 *Opt. Lett.* **31** 2613
[7] Fang L, Du J L, Guo X W, Wang J Q, Zhang Z Y, Luo X G and Du C L 2008 *Chin. Phys.* B **17** 2499
[8] Osvaldo P, Adriano F, Nicola A and Francesco L 2001 *Acc. Chem. Res.* **34** 9
[9] Jacky W and Ben Z T 2005 *Acc. Chem. Res.* **38** 745
[10] Goos F and Hänchen 1947 *Ann. Phys* **1** 333
Goos F and Hänchen 1949 *Ann. Phys* **2** 87
[11] Cao Z Q 2002 *Transfer Matrix Methods in Wave Guiding Optics* (Shanghai: Shanghai Jiao Tong University Press) p13 (in Chinese)
[12] Wang Y P 2006 *Fundamentals of Electromagnetic Fields and Waves* (Xian: Xidian University Press) p206 (in Chinese)